



ORIGINAL

Ali Hajnayeb · Qiao Sun

Study of gear pair vibration caused by random manufacturing errors

Received: 25 March 2021 / Accepted: 1 February 2022 / Published online: 26 February 2022
© The Author(s), under exclusive licence to Springer-Verlag GmbH Germany, part of Springer Nature 2022

Abstract The surface quality and manufacturing errors of gear teeth directly affect their noise and vibration during operation. These errors depend on the quality classes of the gears. The errors or deviations from the ideal surface of a gear have a combination of periodic and random patterns. The available research on the random errors applies numeric methods for solving the governing equations, which are not able to apply arbitrary complicated types of input models in terms of frequency content. They require several iterations and long simulation times especially if the studied system has multiple degrees of freedom, e.g., multi-stage gearboxes. In this paper, a new approach is proposed to determine the effect of random manufacturing errors on the vibrations measured on the bearings of mating gears. This approach is based on finding the spectral density of the response using the excitation spectral density and the frequency response function of the transfer path between an excitation point and a measurement point. For that purpose, a dynamic model for a gear pair and bearings is considered, and the governing equations are derived. Then, an expression for the vibration caused by random error is derived based on the frequency response functions of the system. The numerical values of the expression are then compared with the results obtained from Monte Carlo simulation for a range of values of system parameters. Then, different levels of random manufacturing error are investigated, and the effect of system parameters on the resulting vibration is also studied. The results provide insight into designing new gearboxes based on acceptable levels of vibration and in quantifying the contribution of manufacturing errors in the gearbox to machinery vibration.

Keywords Gear vibrations · Manufacturing error · Random errors · Statistical analysis

Abbreviations

c_{y1}	Bearing damping of the driving gear
c_g	Output shaft damping
$e(t)$	Manufacturing error
k_{y1}	Bearing stiffness of the driving gear
c_g	Output shaft stiffness
m_1	Mass of the driving gear
N_1	Number of teeth of the driving gear
I_b	Mass moment of inertia of the output disk
I_1	Mass moment of inertia of the driving gear

A. Hajnayeb (✉)
Mechanical Engineering Department, Shahid Chamran University of Ahvaz, Postal Code: 6135743337 Ahvaz, Iran
e-mail: a.nayeb@scu.ac.ir

Q. Sun
Department of Mechanical and Manufacturing Engineering, University of Calgary, Calgary, Canada

y_1	Vertical displacement of the driving gear
$Y_1(\omega)$	Fourier transform of y_1
C	Damping matrix of the system
$E(\omega)$	Fourier transform of $e(t)$
K	Stiffness matrix of the system
M_1	Input moment
R_{b1}	Pitch radius of the driving gear
$S_{ee}(\omega)$	Spectral density of an arbitrary manufacturing error
$X(\omega)$	Fourier transform of the vector of state variables
θ_1	Rotation angle of the driving gear
θ_2	Rotation angle of the driven gear
$\Theta_1(\omega)$	Fourier transform of θ_1
$\Theta_m(\omega)$	Fourier transform of θ_m
c_{y2}	Bearing damping of the driven gear
c_p	Input shaft damping
k_t	Meshing stiffness
k_{y2}	Bearing stiffness of the driven gear
k_p	Input shaft stiffness
m_2	Mass of the driven gear
N_2	Number of teeth of the driven gear
I_m	Mass moment of inertia of the motor
I_2	Mass moment of inertia of the driven gear
y_2	Vertical displacement of the driven gear
$Y_2(\omega)$	Fourier transform of y_2
$E[\cdot]$	Mathematical expectation
$H_1(\omega), H_2(\omega)$	The frequency–response functions between the error and the lateral vibrations
M	Mass matrix of the system
M_2	Loading moment
R_{b2}	Pitch radius of the driven gear
$S_{nb}(\omega)$	Spectral density of a narrow-band manufacturing error
ω_1	Maximum frequency content of narrow-band manufacturing error
θ_m	Rotation angle of the motor
θ_b	Rotation angle of the output disk
$\Theta_2(\omega)$	Fourier transform of θ_2
$\Theta_b(\omega)$	Fourier transform of θ_b

1 Introduction

Gear vibrations are mostly caused by several sources including variable meshing stiffness, installation errors, gear faults [1], and manufacturing errors [2]. Vibration caused by variable meshing stiffness is inevitable because the meshing stiffness depends on the number of teeth pairs in contact at a given time, which varies during rotation of the gears. Installation errors and local gear faults can normally be avoided or at least kept to a minimum. Manufacturing errors can be reduced, but there is always a trade-off between reduced manufacturing errors and increased manufacturing costs. Therefore, it is necessary to have an estimate of the effects of manufacturing errors on the gearbox performance and vibrations in order to determine the minimum requirements for manufacturing quality in the design process of the final system assembly.

A group of researchers have been trying to analyze and optimize the gear profile so that the profile errors are minimized [3–8]. Sato et al. [9] studied the effects of gear profile and contact ratio on the rotational vibrations of gears. They validated their simulation results by comparing them with dynamic meshing test results. Tavakoli and Houser [8] and Munro et al. [6] in similar studies used different combinations of tooth and tip reliefs to minimize the static transmission errors of spur gears. Simon [7] provided a method for calculating the optimum values of the tooth tip relief and crowning of gears. Cai and Hayashi [4] found the optimum tooth profile for spur gears so that they have no rotational vibration caused by tooth profile. They showed the effectiveness of the method in simulations. Bonori et al. [10] and Faggioni et al. [5] used a genetic algorithm and a Random–Simplex optimization algorithm, respectively, to minimize the vibrations caused

by gear profile selection. Despite the efforts to eliminate profile errors, there is always manufacturing errors, which lead to discrepancies between the ideal profile and the manufactured one. These errors and their effects can be studied both experimentally and theoretically. For theoretical studies, realistic models of the gear pairs are necessary.

Linear and nonlinear models of gear dynamics have been provided in previous research studies [11, 12]. Velex and Maatar [13] provided a dynamic model for gears in order to study the effects of gear profile and mounting faults on the gear vibrations. Faggioni et al. [14] proposed a nonlinear model for studying the nonlinear vibrations and stability of gear pairs. Masoumi et al. [15] presented a lumped-mass model for a planetary gearbox in order to investigate the nonlinear vibrations and chaos in the gearbox. They considered the effects of backlash and time-varying meshing stiffness in that model. The results showed an induced imbalance in the gearbox. Masoumi et al. [16] in another study, applied a similar model in order to investigate the effects of gear tooth profile and meshing on the vibrations and contact stresses in planetary gearboxes. Unlike the signal-based studies on machinery vibrations [17–21], these gear dynamics models can be combined with the models for gear manufacturing errors, which affect the gear tooth profiles and consequently the vibrations of gearboxes, to improve gearbox design. Therefore, one of the goals of the current research is developing a combined model to analytically study the effects of manufacturing errors.

Because of common random excitation sources in gearboxes, analyzing random vibrations in gearboxes is essential. Random and/or harmonic input torques are considered as one of the sources in this classification. Several research studies, such as [22–25], have investigated the dynamics of gear pairs under random input torques. Another random excitation source is gear manufacturing or profile error. It can cause excessive torsional and also lateral vibrations. Fakhfakh et al. [26] used a 12-degree-of-freedom (DOF) variable-stiffness model to simulate the dynamics of a two-stage gear system. The behavior of the system was studied with and without manufacturing and assembly errors. It was observed that an eccentricity caused an amplitude modulation, but a profile error increased the level of vibration without showing a specific peak in the vibration spectrum. Bonori and Pellicano [3] proposed an approach for analyzing the vibration of a gear pair with profile errors. They applied a 1DOF model for a gear pair considering backlash and variable meshing stiffness. A random distribution was assumed for the profile error. They compared the vibrations of the gear pair in error-free and imperfect cases, and observed that these profile errors could lead to chaotic behavior. Xun et al. [27] studied the dynamics of a planetary gearbox in the case of random tooth profile error. By applying a multiple-scales based stochastic method, they obtained the distributions of dynamic transmission errors (DTEs), which was verified by employing the Monte Carlo method. Based on the results, they concluded that manufacturing precision has significant effects on DTE. Guo and Fang [28] developed a 12-DOF dynamic model to analyze deterministically the effects of manufacturing errors on the DTEs of a helical gear pair. They were able to predict the DTE of the system with experimental validations. Guo and Fang in a similar study [29] performed several statistical analyzes to investigate the effect of different machining accuracy errors on gear vibration. In summary, all the mentioned research works have used numerical methods, which have heavy numerical calculation cost especially in complicated systems with several degrees of freedom and with many modelling details. In the methods based on numerical solutions of differential equations of motion, the inputs are entered in the time domain, but frequency and amplitude distributions of complicated types of random errors are not easy to implement.

The majority of published research on gear vibrations has focused on fault detection and diagnosis using signal-based [19, 30, 31] or model-based [32] approaches without considering the manufacturing errors, but a few works consider that in their models. Park et al. [33] measured the transmission error in a gear set using two encoders. They applied ensemble empirical mode decomposition to the obtained signal, which includes information on gear profile deviations, in order to diagnose gear faults. Dadon et al. [34] numerically simulated the surface interaction between gear teeth in order to investigate the possibility of fault detection in the case of gear manufacturing errors. They investigated the effect of different severity levels of gear tooth profile error. The results showed that the ability to detect faults is degraded in gears with low-quality tooth surfaces, and the robust detection of small faults is not feasible. More investigation is needed in the case of concurrent manufacturing errors and local faults in rotating machinery containing gear transmissions.

Based on the above discussion, in low-accuracy-machined gears, the contribution of the profile random error to gear vibration is significant. It affects the general dynamics and performance of the gear pair, and excessive profile error can possibly lead to a poor estimate of transmission error, an increase in overall vibration, and can make fault detection more challenging. Simulating the effect of manufacturing error on system vibration in the design process can help to reduce the manufacturing costs of the gears while satisfying performance requirements. All the existing theoretical studies on the effects of gear manufacturing error are based on



Fig. 1 Schematic view of an MDOF system, where $f_i(\omega)$ and $w_i(\omega)$ are the i th input and output, respectively

numerical simulations, which take a long time to run and are computationally expensive even for small systems. For more complicated systems and for the purpose of parameter optimization in the presence of manufacturing error, a more efficient method is desirable, especially during the design process where experiments are not possible. Generating the desired types of random errors in current numerical methods is also limited in terms of amplitude and frequency. In this study, a multi-DOF (MDOF) model, including the input and output rotors, and the gears' lateral and torsional vibrations, is prepared. A random pattern of tooth profile error with a known spectral density is considered. By using a frequency domain approach, the vibration levels on the bearings, caused by the random error, are determined. Unlike previous studies, this method provides us with an expression for calculating the vibration level without going through the process of solving the equations of motion, numerically. The results of the proposed method are compared with those obtained by Monte Carlo simulations. After validating the approach, the effects of system parameters on the vibration levels are studied by changing their numerical values over specified ranges. The results show the accuracy of the proposed method and especially its shorter computation time, which gives the results in a few seconds instead of hours of simulations spent on numerical methods.

2 Theory

The spectral density $S_y(\omega)$, of the response of a linear 1DOF system to a random excitation, is defined as $S_y(\omega) = |H(\omega)|^2 S_f(\omega)$ where $S_f(\omega)$ is the spectral density of the input, and $H(\omega)$ is the frequency response function of the system. The mean squared displacement of the response, $E[y^2]$, which is an applied parameter, can be then obtained as $E[y^2] = \int_{-\infty}^{\infty} |H(\omega)|^2 S_f(\omega) d\omega$, as well [35].

In a linear system with multiple degrees of freedom and multiple inputs, such as what is shown in Fig. 1, this approach can be applied by decoupling the governing equations using the mode shapes of the system. In other words, the system is decoupled into m 1DOF systems, and then the mean square displacement of the responses can be obtained for all the new degrees of freedom in the orthogonal coordinate system. A simpler approach is available for obtaining the mean square response in the original coordinate system. It uses the matrix of frequency response functions, $[H(\omega)]$, of the entire system. In the frequency domain, the relation between the inputs and outputs can be written as:

$$\begin{bmatrix} W_1(\omega) \\ W_2(\omega) \\ \vdots \\ W_m(\omega) \end{bmatrix} = [H(\omega)] \begin{bmatrix} F_1(\omega) \\ F_2(\omega) \\ \vdots \\ F_m(\omega) \end{bmatrix} = \begin{bmatrix} H_{11}(\omega) & \cdots & H_{1m}(\omega) \\ \vdots & \ddots & \vdots \\ H_{m1}(\omega) & \cdots & H_{mm}(\omega) \end{bmatrix} \begin{bmatrix} F_1(\omega) \\ F_2(\omega) \\ \vdots \\ F_m(\omega) \end{bmatrix} \quad (1)$$

where $H_{ij}(\omega)$, $W_i(\omega)$ and $F_i(\omega)$ are the ij element of the frequency response function matrix and Fourier transform of the i th output and the i th input, respectively.

Therefore, the mean square of the system response on the n th output caused by the i th input can be obtained from the following equation [36, 37]:

$$E[w_n^2] = \int_{-\infty}^{\infty} |H_{ni}(\omega)|^2 S_{f_i}(\omega) d\omega \quad (2)$$

3 Equations of motion

A system, containing a gear pair, bearings, and input and output rotors, is simplified to an 8-DOF lumped-mass model and shown in Fig. 2. The random manufacturing error is shown as a function of time, $e(t)$, which is connected to the meshing spring and damper in series. The symbols used for stiffness, damping, mass and mass moment of inertia of the system components are k , c , m , and I , respectively. The supporting bearings of

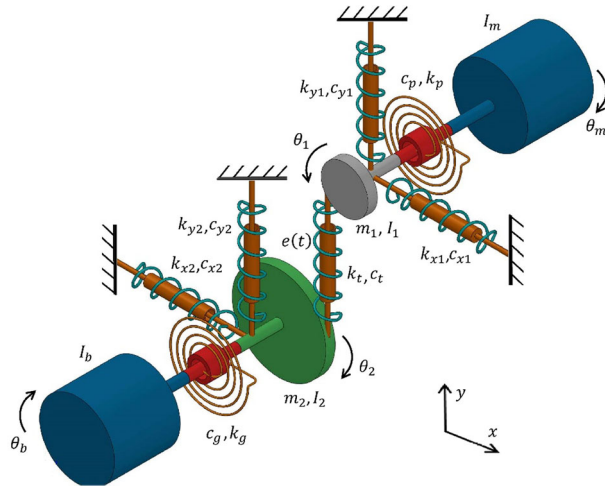


Fig. 2 Schematic view of the gear pair model (reproduced from [38])

the gears are simplified as linear springs and dampers in the y direction, where 1 and 2 in the subscripts refer to the driving and driven gears, respectively. The meshing stiffness and damping are specified with subscript t . The rotational and translational DOFs are shown by θ and y , respectively.

By using Newton’s second law, the equations of motion can be written around the static equilibrium as:

$$m_1 \ddot{y}_1 + c_{y1} \dot{y}_1 + k_{y1} y_1 = -F_k - F_c \tag{3}$$

$$m_2 \ddot{y}_2 + c_{y2} \dot{y}_2 + k_{y2} y_2 = F_k + F_c \tag{4}$$

$$I_1 \ddot{\theta}_1 = k_p (\theta_m - \theta_1) + c_p (\dot{\theta}_m - \dot{\theta}_1) - R_{b1} (F_k + F_c) \tag{5}$$

$$I_2 \ddot{\theta}_2 = R_{b2} (F_k + F_c) - k_g (\theta_2 - \theta_b) - c_g (\dot{\theta}_2 - \dot{\theta}_b) \tag{6}$$

$$I_m \ddot{\theta}_m = M_1 - k_p (\theta_m - \theta_1) - c_p (\dot{\theta}_m - \dot{\theta}_1) \tag{7}$$

$$I_b \ddot{\theta}_b = -M_2 + k_g (\theta_2 - \theta_b) - c_g (\dot{\theta}_2 - \dot{\theta}_b) \tag{8}$$

where

$$F_k = (R_{b1} \theta_1 - R_{b2} \theta_2 + y_1 - y_2 + e(t)) \cdot k_t(t) \tag{9}$$

$$F_c = (R_{b1} \dot{\theta}_1 - R_{b2} \dot{\theta}_2 + \dot{y}_1 - \dot{y}_2 + \dot{e}(t)) \cdot c_t \tag{10}$$

In order to investigate the vibrations caused by manufacturing error, the average value of the meshing stiffness is substituted into the equations of motion (similar to what is done in [26]) to eliminate the contribution of variable meshing stiffness to the vibration level. It is assumed that the vibration amplitudes are low, there is no loss of contact, and meshing frequency does not create primary or parametric resonance. This average value of the meshing stiffness is taken over one period of gear rotation. Therefore, the equations of motion, Eqs. (3)–(13), can be written in matrix form as:

$$\begin{bmatrix} m_1 & 0 & 0 & 0 & 0 & 0 \\ 0 & m_2 & 0 & 0 & 0 & 0 \\ 0 & 0 & I_1 & 0 & 0 & 0 \\ 0 & 0 & 0 & I_2 & 0 & 0 \\ 0 & 0 & 0 & 0 & I_m & 0 \\ 0 & 0 & 0 & 0 & 0 & I_b \end{bmatrix} \begin{bmatrix} \ddot{y}_1 \\ \ddot{y}_2 \\ \ddot{\theta}_1 \\ \ddot{\theta}_2 \\ \ddot{\theta}_m \\ \ddot{\theta}_b \end{bmatrix} + \begin{bmatrix} c_{y1} + c_t & -c_t & c_t R_{b1} & -c_t R_{b2} & 0 & 0 \\ -c_t & c_{y2} + c_t & -c_t R_{b1} & c_t R_{b2} & 0 & 0 \\ c_t R_{b1} & -c_t R_{b1} & c_p + c_t R_{b1}^2 & -c_t R_{b1} R_{b2} & -c_p & 0 \\ -c_t R_{b2} & c_t R_{b2} & -c_t R_{b1} R_{b2} & c_g + c_t R_{b2}^2 & 0 & -c_g \\ 0 & 0 & -c_p & 0 & c_p & 0 \\ 0 & 0 & 0 & -c_g & 0 & c_g \end{bmatrix} \begin{bmatrix} \dot{y}_1 \\ \dot{y}_2 \\ \dot{\theta}_1 \\ \dot{\theta}_2 \\ \dot{\theta}_m \\ \dot{\theta}_b \end{bmatrix}$$

$$+ \begin{bmatrix} k_{y1} + k_t & -k_t & k_t R_{b1} & -k_t R_{b2} & 0 & 0 \\ -k_t & k_{y2} + k_t & -k_t R_{b1} & k_t R_{b2} & 0 & 0 \\ k_t R_{b1} & -k_t R_{b1} & k_p + k_t R_{b1}^2 & -k_t R_{b1} R_{b2} & -k_p & 0 \\ -k_t R_{b2} & k_t R_{b2} & -k_t R_{b1} R_{b2} & k_g + k_t R_{b2}^2 & 0 & -k_g \\ 0 & 0 & -k_p & 0 & k_p & 0 \\ 0 & 0 & 0 & -k_g & 0 & k_g \end{bmatrix} \begin{bmatrix} y_1 \\ y_2 \\ \theta_1 \\ \theta_2 \\ \theta_m \\ \theta_b \end{bmatrix} = \begin{bmatrix} -k_t e(t) - c_t \dot{e}(t) \\ k_t e(t) + c_t \dot{e}(t) \\ -R_{b1} [k_t e(t) + c_t \dot{e}(t)] \\ R_{b1} [k_t e(t) + c_t \dot{e}(t)] \\ 0 \\ 0 \end{bmatrix} \quad (11)$$

Two approaches are used in this research in order to find the solution of these equations in the case of random manufacturing errors. The first one is based on the theory of random vibrations and is analytical. The second approach is the common numerical solution of this set of differential equation using the Runge–Kutta method. In the first approach, the average value of the meshing stiffness is used in Eqs. (11–17), and in the second method, the variable meshing stiffness values from finite element method (FEM), and numerical solutions of Eq. (11) are used. Then, their results will be compared.

Random vibration analysis in the frequency domain needs less calculation time. Moreover, many random excitations are described by their spectral densities and frequency domain distributions. Therefore, after taking a Fourier transform, the above equation can be rewritten as:

$$[-\omega^2 M + \omega IC + K] \begin{bmatrix} \ddot{y}_1 \\ \ddot{y}_2 \\ \Theta_1(\omega) \\ \Theta_2(\omega) \\ \Theta_m(\omega) \\ \Theta_b(\omega) \end{bmatrix} = \begin{bmatrix} -k_t - c_t I \omega \\ k_t + c_t I \omega \\ -R_{b1} [k_t + c_t I \omega] \\ R_{b2} [k_t + c_t I \omega] \\ 0 \\ 0 \end{bmatrix} E(\omega) \quad (12)$$

Then, if Eq. (12) is solved for $[X(\omega)] = [Y_1(\omega) \ Y_2(\omega) \ \Theta_1(\omega) \ \Theta_2(\omega) \ \Theta_m(\omega) \ \Theta_b(\omega)]^T$ one obtains

$$[X(\omega)] = [-\omega^2 M + \omega IC + K]^{-1} [F(\omega)] \quad (13)$$

where $[F(\omega)]$ equals to the right-hand side of Eq. (12). Then, the first two elements of $[X(\omega)]$ can be obtained from Eq. (13) as:

$$Y_1(\omega) = H_1(\omega) E(\omega) \quad (14)$$

and

$$Y_2(\omega) = H_2(\omega) E(\omega) \quad (15)$$

They represent the Fourier transform of the lateral vibrations of the bearings in the y direction caused by static transmission error or, in other words, manufacturing error. Because of the 6 degrees of freedom of the system, the expressions obtained for frequency–response functions, $H_1(\omega)$ and $H_2(\omega)$, are lengthy and are not written here. If the manufacturing error has a general spectral density of $S_{ee}(\omega)$, the mean square displacement of the response, caused by that error on the bearing supporting the driving gear, can be obtained from the following equation [37]:

$$E[y_1^2(t)] = \int_{-\infty}^{\infty} |H_1(\omega)|^2 S_{ee}(\omega) d\omega \quad (16)$$

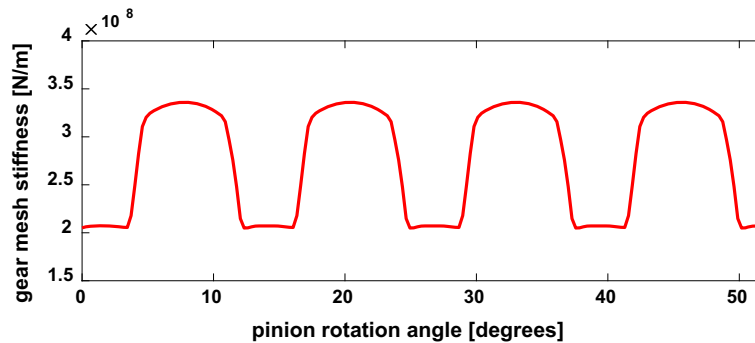
Equation (16) is used in cases where the frequency of error is not limited to a specific range. In most of cases, this type of error is assumed to be low-frequency noise with a frequency limit. For a random input with spectral density of $S_{nb}(\omega)$ with an upper bound of ω_1 , the mean square of the response can be obtained from the following equation:

$$E[y_1^2(t)] = \int_{-\omega_1}^{\omega_1} |H_1(\omega)|^2 S_{nb}(\omega) d\omega \quad (17)$$

Based on Eq. (17), if the spectral density of the error is known, the mean square of the response can be calculated.

Table 1 The values of the system parameters

Parameter	Value	Parameter	Value
c_g	300 [N.m.s/rad]	c_p	300 [N.m.s/rad]
c_{y1}	4000 [N.s/m]	c_{y2}	4000 [N.s/m]
c_t	1000 [N.s/m]	Gear module	3 [mm]
I_1	0.001 [kg.m ²]	I_2	0.01 [kg.m ²]
I_b	0.5 [kg.m ²]	I_m	0.6 [kg.m ²]
k_p	4e7 [N.m/rad]	k_g	4e7 [N.m/rad]
k_{y1}	1e7 [N/m]	k_{y2}	1e7 [N/m]
\bar{k}_t	2.75e8 [N.m/rad]	Backlash	0.04 [mm]
R_{b1}	87 [mm]	R_{b2}	147 [mm]
m_1	0.9 [kg]	m_2	2.6 [kg]
N_1	29	N_2	49
Tooth width	20 [mm]	Pressure angle	25 [degrees]

**Fig. 3** The variable gear meshing stiffness used in this study

4 Numerical results

As a case study, the numerical values of the system parameters are assumed as given in Table 1. In order to be able to compare the results, the gear pair analyzed in this section has the same properties as the one analyzed in [39]. The gears used in the system have parabolic tip relief, and an amplitude of 0.01 mm is assumed for modification. The numerical values of other parameters of the gearbox are provided in Table 1.

The value of meshing stiffness varies over time, but in the proposed method, the average value of k_t over a cycle of its variation, which is denoted as \bar{k}_t , is substituted into the matrix form of equations of motion [26]. This average value is obtained by averaging the values obtained during a single cycle of variation of meshing stiffness obtained from a FEM model [39]. A number of these cycles are shown in Fig. 3.

Based on the numerical values provided in Table 1, the function $H_1(\omega)$ is determined. Then, by applying Eq. (17), the mean square value of the lateral vibrations of the bearing of the driving gear can be obtained for a random tooth profile error with a known spectral density.

In this section, the effects of different parameters on the resulting vibrations are studied by changing the numerical values of the parameters and plotting the corresponding values of vibration levels. Before that, the model equations and the obtained results have to be validated. In order to validate the results of the proposed method, a Monte Carlo simulation is conducted in Simulink. For that purpose, the equations of motion are written in the state-space form, and then they are reproduced in Simulink by using gain, summation, and integrator blocks. For solving the equations in Simulink, the ODE23s solver has been selected, which applies a variable-step Runge–Kutta method. For conducting the simulations, a model for the random manufacturing error is also needed. The random manufacturing error is mainly determined by the quality class of the gears. In this study, the quality classes are assumed based on the ISO 1328 standard mentioned in [40], where 12 quality classes are considered for gears. Based on this standard, the standard deviations of the random part of the gear profile manufacturing error of classes 7 and 9 are $1\ \mu\text{m}$ and $2.5\ \mu\text{m}$, respectively. A third value of zero error (for the ideal condition), in addition to these two error values, is considered in our manuscript for the numerical simulation and comparison. The selected values of standard deviation for this research are of the same order as $1\ \mu\text{m}$, $2.24\ \mu\text{m}$, and $3.16\ \mu\text{m}$, used in the study conducted in [41]. In that research, the theoretical random error

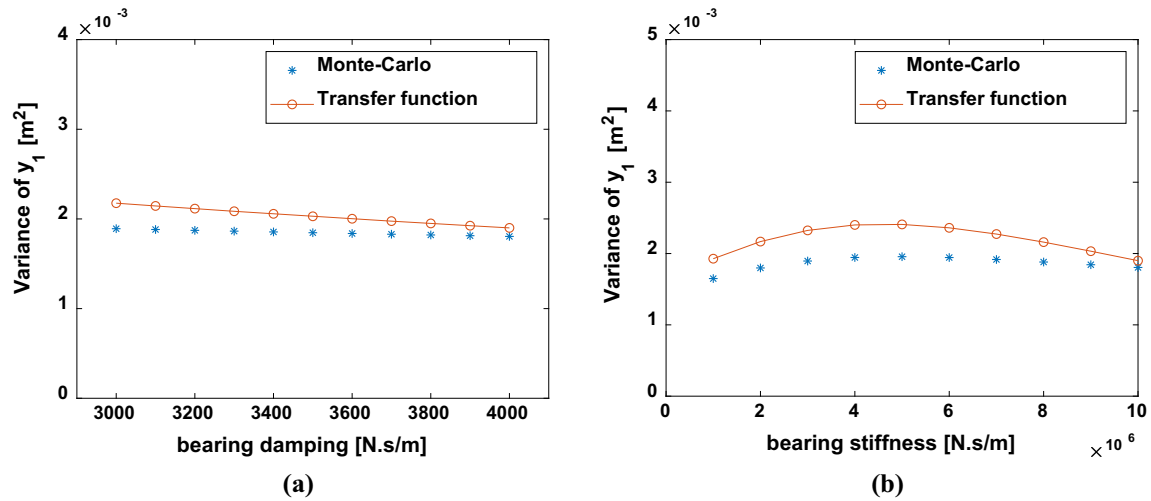


Fig. 4 Vibration level of the driving bearing for different values of bearing **a** damping, and **b** stiffness

is compared with the measured errors on a gear test setup. The comparison showed good agreement between them. The assumed errors have similar ranges to the approximate random error assumed in [39], too. Therefore, the properties of the applied transmission error are considered to be the same as the properties of these profile errors. Similar to [41], a random model is assumed for the transmission error. It is assumed that the random manufacturing error is a band-limited white signal and has a uniform power spectral density (PSD) over the frequency range of zero to 200 Hz.

First, a uniform hypothetical PSD of $10^{-6} [\text{m}^2/(\text{rad/s})]$ over the frequency range of zero to 200 Hz is assumed for the random manufacturing error to compare the results of the analytical method and the Monte Carlo simulation. This high value is selected so that the manufacturing error becomes the main source of excitation in both methods. In Fig. 4, the results of the proposed analytical method and Monte Carlo simulation are compared for the case of standard deviation of manufacturing error PSD of $10^{-6} [\text{m}^2/(\text{rad/s})]$. In that figure, the vibration caused by the manufacturing error is shown for different values of bearing stiffness and damping of the driving gear bearing. They show close agreement for different values of the studied parameters. Therefore, in the next step, the practical values of manufacturing errors will be applied.

After validating the models, we study the contribution of manufacturing error to the total vibration of the rotating gears in order to compare it with the baseline level of vibration caused by time variations in meshing stiffness. As stated before, the vibration caused in gear systems by the variable meshing stiffness is inevitable; however, the manufacturing quality is a controllable source of vibration. We apply different levels of manufacturing error in the model, as used in the previous step. A variable meshing stiffness obtained from FEM is applied using a look-up table in Simulink (Fig. 5a), which is composed of the values of one cycle out of several cycles shown in Fig. 3, earlier. The number of teeth of the driving and driven gears are 29 and 49, respectively. Therefore, for an input rotational speed of 1800 RPM, the frequency of stiffness cycles would be $19 \times 30 = 570\text{Hz}$, which is considered in the model.

An input torque of 200 N.m and a loading torque of 326.3 N.m are also applied to keep the teeth loaded and induce vibrations in the gears during the simulation. First, the vibration level on the bearing of the driving gear is studied without any manufacturing error. Then, manufacturing errors with the same frequency band but different standard deviations (SDs) of 1-m and 2.5-m are applied. Parts of the generated signals are shown in Fig. 5b for those two cases.

In Fig. 6a, the bearing vibration in the case of $SD = 1\text{-m}$ for part of the simulation is plotted in the frequency domain. The first harmonic of the gear mesh frequency (870 Hz) in addition to a natural frequency of about 80.7Hz is observed in that figure. The undamped natural frequencies of the system can be obtained by setting the damping and manufacturing error in Eq. (14) to zero. In other words, the natural frequencies can be calculated by finding the square root of the eigenvalues of $M^{-1}K$ using mass and stiffness matrices [42] provided in Eq. (11) and the numerical values provided in Table 1. A complete list of the system natural frequencies is provided in Table 2. The first nonzero natural frequency of the system is obtained as 80.7Hz. Since the excitation is white noise, the natural frequencies of the system in its frequency band are excited as what was seen in Fig. 6a. Moreover, because the averaged spectrum is shown in this figure, the expected

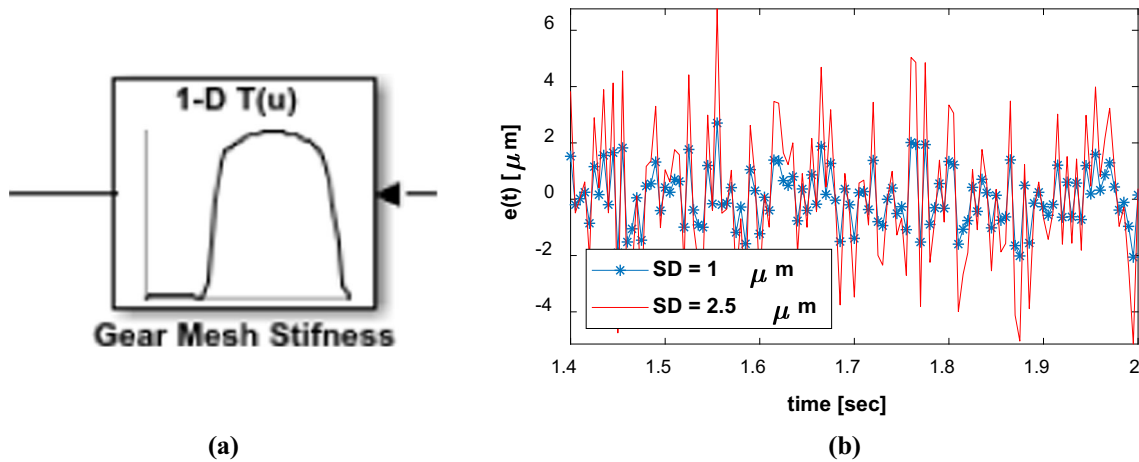


Fig. 5 **a** Look-up table used in the Simulink model for simulating variable meshing stiffness. **b** Random manufacturing errors

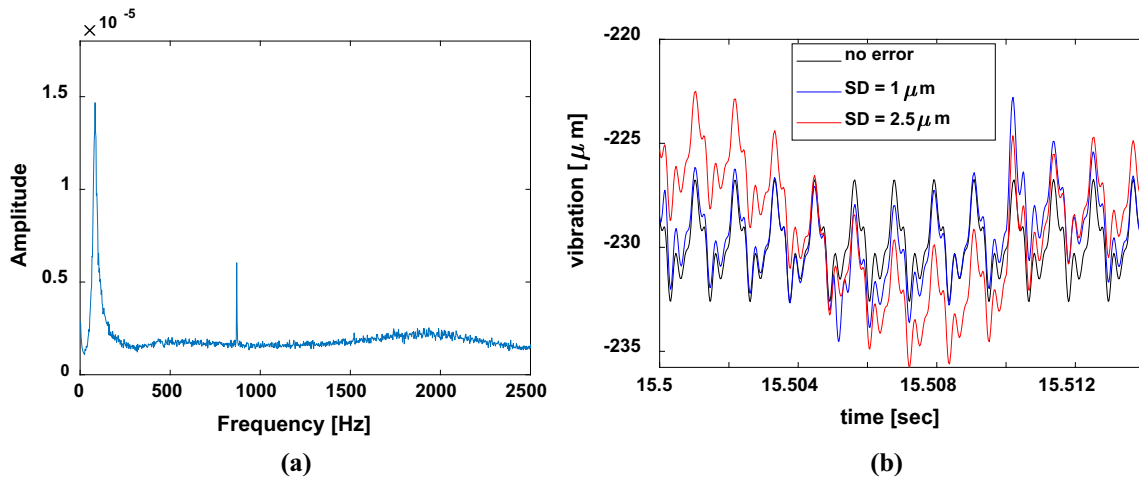


Fig. 6 **a** The spectrum of vibrations of the bearing of the driving gear in frequency domain for $SD = 2.5 \mu m$. **b** Comparing bearing vibration signals for three different levels of manufacturing error

Table 2 The system natural frequencies

Natural frequency number	1	2	3	4	5	6
Value [Hz]	0	80.7	381.6	3026.7	10,890.4	32,694.2

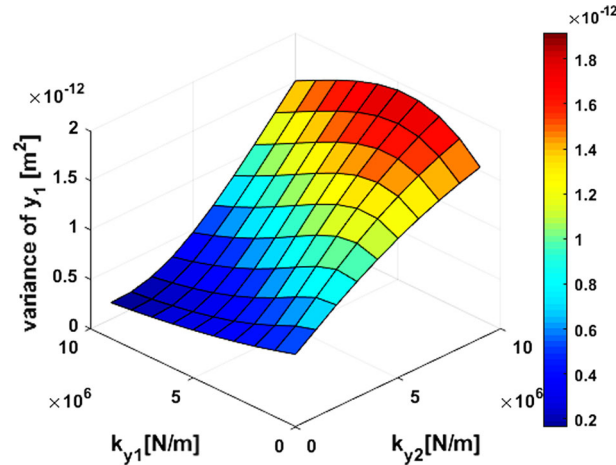
background noise caused by the random manufacturing error is mostly canceled out and is not observed in this figure. The random vibrations are canceled out in almost all the frequencies except for the first natural frequency of the system and the gear meshing frequencies.

In Fig. 6b, a time span of the steady-state signals (after the transient part is damped out) of bearing displacement over time are compared in the three mentioned cases. The bearing vibration signal without any manufacturing errors is plotted in black. Only the vibrations caused by the change in meshing stiffness are observed in that signal. The blue and also the red signals are obtained by applying band-limited random error. The first natural frequency is excited and observed as a harmonic component in the time domain as well as the frequency domain. The random vibrations are also observed in the time signal.

The results of applying different levels of manufacturing error are shown in Table 3. It shows how much the errors can increase the SD and variance of vibrations on the bearing of the driving gear. It can be seen how the variance and SD of vibrations change in cases with constant meshing stiffness and the cases with

Table 3 The values of errors and system vibrations in cases of variable and constant meshing stiffness

Meshing stiffness	SD of manufacturing error (μm)	Bearing vibration SD (μm)	Bearing vibration variance (μm)	Frequency range (Hz)
Variable	0	3.146	9.898	[0, 200]
	1	3.217	10.347	[0, 200]
	2.5	3.825	14.631	[0, 200]
Constant (average value)	1	1.171	1.372	[0, 200]
	2.5	2.927	8.570	[0, 200]

**Fig. 7** Vibration level of the driving bearing for different values of error and bearing stiffness

variable meshing stiffness. The total vibration level in each case is influenced by the variable stiffness and also manufacturing error.

After validating the initial results, the effects of different system parameters are studied using Eq. (20). A white signal with a variance of 10^{-12}m^2 , which is equivalent to a uniform power spectral density (PSD) of $\frac{10^{-12}}{2\pi \times 200} [\text{m}^2/(\text{rad/s})]$ with the same frequency range as before, is assumed for the manufacturing error. Based on this PSD, it is known that the error has a SD of 1 μm . In Fig. 7, the vibration level of the bearing is plotted for different values of bearing stiffnesses. It shows that in the studied range of values, increasing the bearing stiffnesses of the driving gear, k_{y1} , can reduce or increase the vibration level of the driving gear bearing, while increasing the bearing stiffness of the driven gear k_{y2} increases the vibration level.

In Fig. 8, the vibration level of the same bearing is plotted for different bearing damping values. It shows decreases in the vibration level by increasing the damping values at either of the bearings, which was to be expected. Next, the stiffnesses of the shafts between the motor and the driving gear and between the driven gear and the load are changed, and the results are shown in Fig. 9. This figure shows that the vibration level for most of that range of stiffness values is not noticeably sensitive to these shaft stiffnesses.

5 Conclusions

In this research work, a simplified model of a gear pair was used to study the vibrations caused by random manufacturing errors in the tooth profiles of gears. The transfer functions between the excitation source, which is the manufacturing error, and the common measurement locations were obtained. The equations for obtaining the mean square of translational vibrations of a point on the bearing of one of the gears in the case of a limited-frequency random error were extracted as an example. The results were validated by comparing them with Monte Carlo simulation results. Then, the total vibration level was studied for different severities of manufacturing error. The comparison between the vibration levels in these cases verified the contribution of the manufacturing error to total vibration of the system. Finally, the faster computational speed of the proposed method made it possible to conduct a study on the effect of changing system parameters on the vibrations. The vibrations caused by the manufacturing error were also predicted for different values of system parameters,

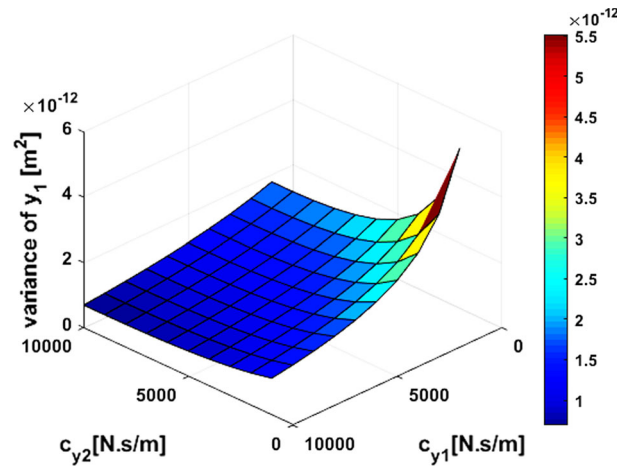


Fig. 8 Vibration level of the driving bearing for different values of damping in gear bearings

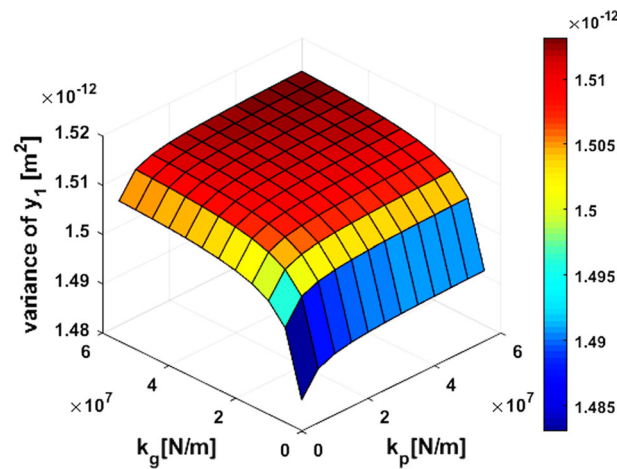


Fig. 9 Vibration level of the driving bearing for different values of input and output shaft stiffnesses

which showed that the overall vibration levels were sensitive to changes in the values of system parameters. The results can be used for designing gearboxes and predicting the normal vibration levels of machines for vibration trending and condition monitoring in cases where random noticeable manufacturing errors may be present. This method can easily be used to study the effect of random manufacturing error on the torsional vibrations of the system using the related transfer functions. Compared to the simulations based on numerical solutions of equations of motion, the proposed approach reduces the computational time of simulations in the design process significantly.

Acknowledgements This research received no specific grant from any funding agency in the public, commercial, or not-for-profit sectors.

Declaration

Conflict of interest The authors declare no conflict of interest in preparing this article.

References

1. Gelman, L., Chandra, N.H., Kurosz, R., Pellicano, F., Barbieri, M., Zippo, A.: Novel spectral kurtosis technology for adaptive vibration condition monitoring of multi-stage gearboxes. *Insight-Non-Destr. Test. Cond. Monitor.* **58**, 409–416 (2016)
2. Harris, S.L.: Dynamic loads on the teeth of spur gears. *Proc. Inst. Mech. Eng.* **172**, 87–112 (1958)

3. Bonori, G., Pellicano, F.: Non-smooth dynamics of spur gears with manufacturing errors. *J. Sound Vib.* **306**, 271–283 (2007)
4. Cai, Y., Hayashi, T.: The optimum modification of tooth profile for a pair of spur gears to make its rotational vibration equal zero. In: *International Design Engineering Technical Conferences and Computers and Information in Engineering Conference: American Society of Mechanical Engineers*. pp. 453–60 (1992).
5. Faggioni, M., Samani, F.S., Bertacchi, G., Pellicano, F.: Dynamic optimization of spur gears. *Mech. Mach. Theory* **46**, 544–557 (2011)
6. Munro, R., Yildirim, N., Hall, D.: Optimum profile relief and transmission error in spur gears. *Gearbox Noise Vib.* 35–42 (1990)
7. Simon, V.: Optimal tooth modifications for spur and helical gears. *J. Mech. Trans. Automation*. **111**(4), 611–615 (1989). <https://doi.org/10.1115/1.3259044>
8. Tavakoli, M., Houser, D.: Optimum profile modifications for the minimization of static transmission errors of spur gears. (1986).
9. Sato, T., Umezawa, K., Ishikawa, J.: Effects of contact ratio and profile correction on gear rotational vibration. *Bull. JSME*. **26**, 2010–2016 (1983)
10. Bonori, G., Barbieri, M., Pellicano, F.: Optimum profile modifications of spur gears by means of genetic algorithms. *J. Sound Vib.* **313**, 603–616 (2008)
11. Korca, Z.: An overview of mathematical models used in gear dynamics. *Rom. J. Acoust. Vib.* **4**, 43–50 (2007)
12. Özgüven, H.N., Houser, D.R.: Mathematical models used in gear dynamics—a review. *J. Sound Vib.* **121**, 383–411 (1988)
13. Velez, P., Maatar, M.: A mathematical model for analyzing the influence of shape deviations and mounting errors on gear dynamic behaviour. *J. Sound Vib.* **191**, 629–660 (1996)
14. Faggioni, M., Avramov, K., Pellicano, F., Reshetnikova, S.: Nonlinear oscillations and stability of gear pair. *J. Mech. Eng.* **6**(4), 40–45 (2005)
15. Masoumi, A., Pellicano, F., Samani, F.S., Barbieri, M.: Symmetry breaking and chaos-induced imbalance in planetary gears. *Nonlinear Dyn.* **80**, 561–582 (2015)
16. Masoumi, A., Barbieri, M., Pellicano, F., Zippo, A., Strozzi, M.: Dynamic imbalance of high-speed planetary gears. *Int. J. Cond. Monit.* **7**, 2–6 (2017)
17. Azizi, R., Attaran, B., Hajnayeb, A., Ghanbarzadeh, A., Changizian, M.: Improving accuracy of cavitation severity detection in centrifugal pumps using a hybrid feature selection technique. *Measurement* **108**, 9–17 (2017)
18. Hajnayeb, A.: Cavitation analysis in centrifugal pumps based on vibration bispectrum and transfer learning. *Shock Vib.* **2021** (2021). <https://doi.org/10.1155/2021/6988949>
19. Hajnayeb, A., Ghasemloonia, A., Khadem, S., Moradi, M.: Application and comparison of an ANN-based feature selection method and the genetic algorithm in gearbox fault diagnosis. *Expert Syst. Appl.* **38**, 10205–10209 (2011)
20. Hajnayeb, A., Khadem, S., Moradi, M.: Design and implementation of an automatic condition-monitoring expert system for ball-bearing fault detection. *Ind. Lubr. Tribol.* **60**(2), 93–100 (2008) <https://doi.org/10.1108/00368790810858395>
21. Hajnayeb, A., Shirazi, K.H., Aghaamiri, R.: Vibration measurement for crack and rub detection in rotors. *Metrol. Meas. Syst.* **27**(1), 65–80 (2020) <https://doi.org/10.24425/mms.2020.131719>
22. Fang, Y., Zuo, M.J., Li, Y.: Efficient analytical method to obtain the responses of a gear model with stochastic load and stochastic friction. In: *IOP Conference Series: Materials Science and Engineering: IOP Publishing*. p. 012063 (2019)
23. Fang, Y., Zuo, M.J., Li, Y.: Investigation of gear dynamic characteristics under stochastic external excitations. In: *IOP Conference Series: Materials Science and Engineering: IOP Publishing*. p. 012013 (2019)
24. Wang, J., Wang, H., Guo, L.: Analysis of effect of random perturbation on dynamic response of gear transmission system. *Chaos Solitons Fractals* **68**, 78–88 (2014)
25. Zhang, Y., Spanos, P.D.: Efficient response determination of a MDOF gear model subject to combined periodic and stochastic excitations. *Int. J. Non-Linear Mech.* **120**, 103378 (2020)
26. Fakhfakh, T., Walha, L., Louati, J., Haddar, M.: Effect of manufacturing and assembly defects on two-stage gear systems vibration. *Int. J. Adv. Manuf. Technol.* **29**, 1008–1018 (2006)
27. Xun, C., Long, X., Hua, H.: Effects of random tooth profile errors on the dynamic behaviors of planetary gears. *J. Sound Vib.* **415**, 91–110 (2018)
28. Guo, F., Fang, Z.: Experimental and theoretical study of gear dynamical transmission characteristic considering measured manufacturing errors. *Shock Vib.* **2018** (2018). <https://doi.org/10.1155/2018/9645453>
29. Guo, F., Fang, Z.: The statistical analysis of the dynamic performance of a gear system considering random manufacturing errors under different levels of machining precision. *Proc. Inst. Mech. Eng. Part K J. Multi-body Dyn.* **234**, 3–18 (2019)
30. Feng, Z., Lin, X., Zuo, M.J.: Joint amplitude and frequency demodulation analysis based on intrinsic time-scale decomposition for planetary gearbox fault diagnosis. *Mech. Syst. Signal Process.* **72**, 223–240 (2016)
31. Qi, Y., Shen, C., Shi, J., Huang, W., Zhu, Z.: Adaptive morphological feature extraction and support vector regressive classification for gearbox fault diagnosis. In: *2019 IEEE/ASME International Conference on Advanced Intelligent Mechatronics (AIM): IEEE*. p. 868–72 (2019).
32. Liang, X., Zuo, M.J., Feng, Z.: Dynamic modeling of gearbox faults: a review. *Mech. Syst. Signal Process.* **98**, 852–876 (2018)
33. Park, S., Kim, S., Choi, J.-H.: Gear fault diagnosis using transmission error and ensemble empirical mode decomposition. *Mech. Syst. Signal Process.* **108**, 262–275 (2018)
34. Dadon, I., Koren, N., Klein, R., Lipsett, M., Bortman, J.: Impact of gear tooth surface quality on detection of local faults. *Eng. Fail. Anal.* **108**, 104291 (2020)
35. Newland, D.E.: *An Introduction to Random Vibrations, Spectral & Wavelet Analysis*. Courier Corporation, North Chelmsford (2012)
36. Bendat, J.S., Piersol, A.G.: *Random Data: Analysis and Measurement Procedures*. Wiley, Hoboken (2011)
37. Roberts, J.B., Spanos, P.D.: *Random Vibration and Statistical Linearization*. Courier Corporation, North Chelmsford (2003)
38. Liang, X.-H., Liu, Z.-L., Pan, J., Zuo, M.J.: Spur gear tooth pitting propagation assessment using model-based analysis. *Chin. J. Mech. Eng.* **30**, 1369–1382 (2017)

39. Lei, D., Kong, X., Chen, S., Tang, J., Hu, Z.: Numerical and experimental investigation of a spur gear pair with unloaded static transmission error. *Eng. Comput.* **38**(6), 2461–2480 (2020). <https://doi.org/10.1108/EC-02-2020-0072>
40. Maitra, G.M.: *Handbook of Gear Design*. Tata McGraw-Hill Education, New York (1994)
41. Wang, Y., Zhang, W.: Stochastic vibration model of gear transmission systems considering speed-dependent random errors. *Nonlinear Dyn.* **17**, 187–203 (1998)
42. Hajnayeb, A., Fernando, J.S., Sun, Q.: Effects of vehicle driveline parameters and clutch judder on gearbox vibrations. *Proc. Inst. Mech. Eng. Part D J. Automob. Eng.* **236**, 84–98 (2021)

Publisher's Note Springer Nature remains neutral with regard to jurisdictional claims in published maps and institutional affiliations.